

DOI: 10.1002/cbic.201300164

Fluorescent THF-Based Fructose Analogue Exhibits Fructose-Dependent Uptake

Marina Tanasova,^[a] Matthew Plutschack,^[b] Megan E. Muroski,^[b] Shana J. Sturla,^[a] Geoffrey F. Strouse,^[b] and D. Tyler McQuade^{*[b, c]}

Recent publications suggest that high dietary fructose might play a significant role in cancer metabolism and can exacerbate a number of aspects of metabolic syndrome. Addressing the role that fructose plays in human health is a controversial question and requires a detailed understanding of many factors including the mechanism of fructose transport into healthy and diseased cells. Fructose transport into cells is thought to be largely mediated by the passive hexose transporters Glut2 and Glut5. To date, no probes that can be selec-

tively transported by one of these enzymes but not by the other have been identified. The data presented here indicate that, in MCF-7 cells, a 1-amino-2,5-anhydro-D-mannitol-based fluorescent NBDM probe is transported twice as efficiently as fructose and that this takes place with the aid of Glut5. Its Glut5 specificity and differential uptake in cancer cells and in normal cells suggest this NBDM probe as a potentially useful tool for cross-cell-line correlation of Glut5 transport activity.

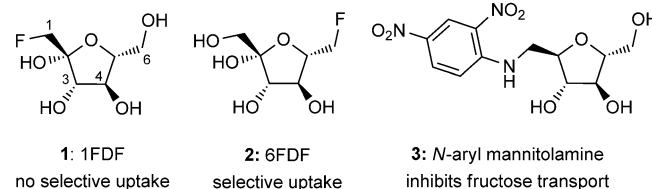
Introduction

Cells must selectively take up nutrients such as carbohydrates to fuel metabolic processes. Eukaryotic cells facilitate uptake by having both passive and active hexose transporters to acquire simple carbohydrates from their environment. Hexose uptake plays a significant role in a wide range of human disease states including diabetes, obesity, gout, cancer, sclerosis, and Alzheimer's.^[1]

There are two classes of hexose transporters: active sodium-coupled glucose transporters (SGLTs) and passive glucose transporters (Gluts). The Gluts (Gluts1–14) facilitate uptake of glucose, fructose, galactose, and other nutrients.^[2] Glut1 is the major glucose transporter expressed in all tissues. Glut5 and Glut2 are the major fructose transporters, although Glut2 also mediates influx of glucose, galactose, and glucosamine.^[3] Recently, a renewed interest has emerged in the Gluts as targets for probes, as a result of increased saccharide consumption in cells in transition from normal to neoplastic states.^[4]

Glucose analogues such as 2-deoxy-2-(¹⁸F)fluoro-D-glucose are established PET imaging agents.^[5] Now, however, fructose

analogues and fructose uptake inhibitors are also becoming targets of interest, due to fructose's potential role in aggressive tumor growth and metabolic syndrome.^[1b] The first 1-deoxy-1-(¹⁸F)fluoro-fructose analogue (compound **1**, Scheme 1), produced by Maeda and co-workers, showed little specificity for



Scheme 1. Modified fructose analogues as fructose-transport-specific probes.

tissue expressing fructose transporters.^[6] Later, Holman and co-workers established that the Glut5 transporter has a preference for cyclic furanose analogues of fructose^[7] and displays highly specific recognition of the C1 and C3 fructofuranose hydroxy groups.^[8] On the basis of Holman's observations, West and Cheeseman created fructose analogue **2** (Scheme 1), which exhibits effective uptake into cancer cells. The C6 substitution prevented intracellular metabolism, however, and the probe readily diffused out of the cells.^[9]

C1- or C3-modification of fructose was poorly tolerated by the receptor, but substitution, epimerization, or elimination of the C2 hydroxy group produced fructose analogues, including 2,5-anhydro-D-mannitol, with affinities for Glut5 similar to that of fructose.^[8] Later, *N*-aryl conjugates of 2,5-anhydro-D-mannitol, such as **3** (Scheme 1), were found to inhibit fructose uptake effectively, and 1-amino-2,5-anhydro-D-mannitol was

[a] Dr. M. Tanasova, Prof. S. J. Sturla

Department of Health Sciences and Technology
Swiss Federal Institute of Technology (ETH Zürich)
Schmelzbergstrasse 9, 8092 Zürich (Switzerland)

[b] M. Plutschack, M. E. Muroski, Prof. G. F. Strouse, Prof. D. T. McQuade

Department of Chemistry and Biochemistry, Florida State University
95 Chieftan Way, Tallahassee, FL 32306-4390 (USA)
E-mail: mcquade@chem.fsu.edu

[c] Prof. D. T. McQuade

Department for Biomolecular Systems
Max Planck Institute for Colloids and Interfaces
Am Mühlenberg 1, 14476 Potsdam (Germany)
E-mail: tyler.mcquade@mpikg.mpg.de

 Supporting information for this article is available on the WWW under <http://dx.doi.org/10.1002/cbic.201300164>.

used to construct biotin-tagged affinity probes.^[10] The best-affinity probe captured Glut5 from CHO cells overexpressing the protein, but the mechanism of fructose uptake inhibition observed with *N*-aryl conjugates of 1-amino-2,5-anhydro-*D*-mannitol or the selectivity of 1-amino-2,5-anhydro-*D*-mannitol towards particular transporter types have not yet been assessed. We hypothesized that the observed drop in fructose uptake is due to the competitive passage of 1-amino-2,5-anhydro-*D*-mannitol into the cells. To test our hypothesis, we synthesized fluorescently labeled 1-amino-2,5-anhydro-*D*-mannitol and evaluated its uptake relative to the corresponding fructosamine conjugate, recently reported by Gambhir and co-workers. We found that our probe enters the cell more avidly than fructose and does so exclusively through fructose-specific transport.

Results and Discussion

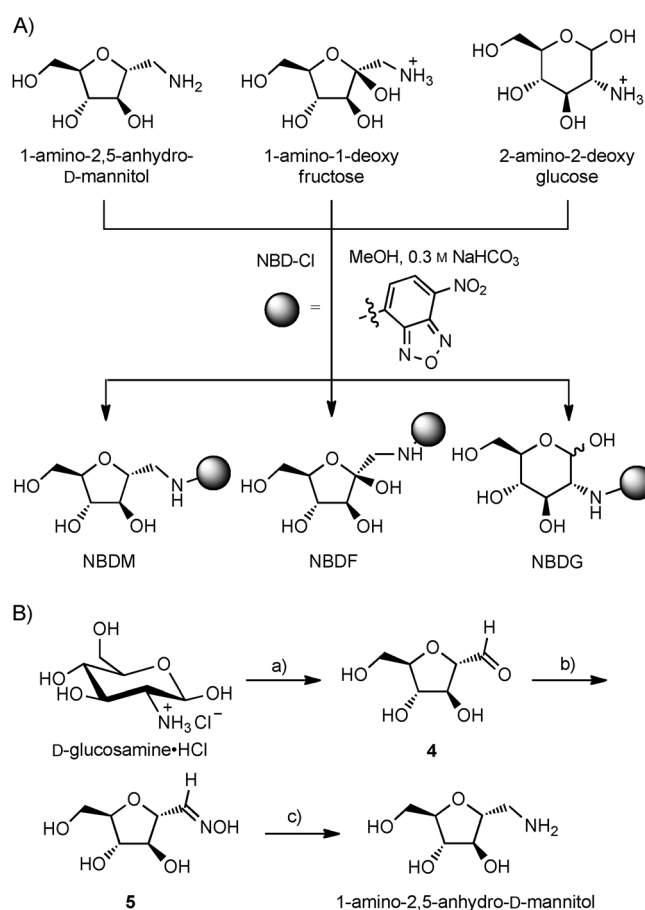
Synthesis of fluorescent conjugates

Advances in cell imaging^[11] enable the use of fluorescent probes for studying the mechanism of carbohydrate uptake. Of the different fluorophores available, 7-nitro-2,1,3-benzoxadiazole (NBD) has been shown to pass into cells when conjugated to glucosamine or fructosamine (NBDG and NBDF, Scheme 2A), and is thought to be transported through Gluts.^[12] Accordingly, we hypothesized that a 1-amino-2,5-anhydro-*D*-mannitol-NBD conjugate (NBDM, Scheme 2A) would be a suitable fluorescent probe for evaluating whether 1-amino-2,5-anhydro-*D*-mannitol is transported and whether the observed uptake is inhibited by natural sugars.

Three fructose analogues (Scheme 2) for comparative uptake studies were synthesized by reported procedures^[12c] and subsequently conjugated to NBDCl. Fructosamine was synthesized from glucose by the procedure reported by Auger et al.^[13]

1-Amino-2,5-anhydro-*D*-mannitol was synthesized from glucosamine by a modified procedure.^[14] Claustre et al. used an acidic resin to produce HONO in situ, and carried out a subsequent neutralization with basic ion-exchange resin. Our modifications to the method include exchanging the chloride ion of the glucosamine-HCl salt with nitrite, which then allows the reaction to occur without excess acid. Thus, by our modified synthesis, the Amberlite IRA-900 nitrite form was prepared by passing NaNO₂ solution through the column until the AgNO₃ test for chloride ions was negative, followed by removal of the residual NaNO₂ by an aqueous wash. Passing the solution of *D*-glucosamine-HCl through Amberlite IRA-900 nitrite provided **4** quantitatively (Scheme 2B). The synthesis was completed by forming the oxime **5**, followed by hydrogenolysis.^[14]

1-Amino-1-deoxyfructose was synthesized through Amadori rearrangement of *D*-glucose with dibenzylamine, followed by hydrogenolysis of the benzyl groups.^[13]



Scheme 2. A) Fluorescent conjugates for uptake studies. B) Synthesis of 1-amino-2,5-anhydro-*D*-mannitol from *D*-glucosamine hydrochloride. a) Amberlite IRA-900 nitrite form, H₂O; b) hydroxylamine-HCl, NaOAc, MeOH; c) Pd/C, H₂, MeOH, 92%.

Competitive uptake of NBDM as a fructose uptake inhibitory mechanism

Transport of each analogue (NBDM, NBDF, and NBDG) was evaluated with breast cancer MCF7 cells, which have previously been observed to exhibit enhanced fructose uptake.^[12c, 15] Whereas NBD chloride is not fluorescent, its amino conjugate emits at 538 nm, where autofluorescence is to be expected. To ensure a clean readout of NBDM-induced cell fluorescence, the magnitude of transport was measured by spectral confocal microscopy so that background fluorescence could be spectrally resolved from the dye signal and each cell could be normalized to its individual autofluorescence. The resulting data are reported as Gained Fluorescence.

Treating MCF7 cells with 10 μM NBDM enhanced cell fluorescence, thus suggesting that the probe is either taken up by the cell or is associated with cell membrane (Figure 1A). A Z-stack analysis of treated cells was used to identify localization of NBD probes. Cell membrane staining with wheat germ agglutinin/Alexa Fluor 594 was used to delineate internalization of the dye clearly. Distinguishing the cell surface from the cytosol allowed rejection of probe electrostatic association with the cell surface and showed that NBDM is effectively internal-

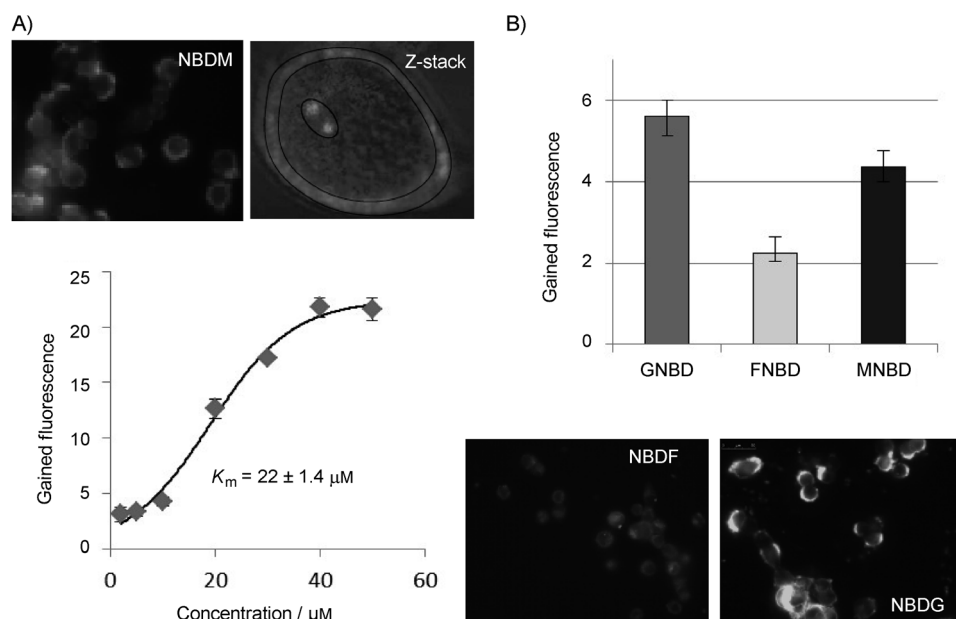


Figure 1. Uptake of NBD conjugates in MCF7 cells. A) NBDM uptake in MCF7 cells (total cell fluorescence and single-cell Z-stack) is dose-dependent. The single-cell imaging (Z-stack) was performed with a Nikon TE2000-E2 Eclipse microscope (Nikon Instruments, Inc., Melville, NY, USA), imaged with a CoolSNAP HQ2 monochrome camera (Photometrics) and a 40 \times lens, and analyzed with Nikon NIS Elements software—the outer ring of the Z-stack, highlighted by the drawn rings, appears red and the inner circle is green, from the wheat germ agglutinin/Alexa Fluor 594 and NBDM, respectively. B) Comparative uptake of glucosamine, fructosamine, and manitolamine conjugates and fluorescent images of MCF7 cells treated with NBDF and NBDG. Fluorescence was measured with an eGFP filter (excitation 450/490 nm, emission 515/565 nm) after treatment of cells with 10 μM conjugate for 15 min (gray regions appear green in color images). Data were quantified in Leica Application Suite software as the sums of intensity for selected cells (10–15). Gained Fluorescence (fold increase) was calculated with respect to cell autofluorescence.

ized by the cell and accumulates in cytosol. We also observed that NBDM uptake is dose-dependent and that MCF7 cells become saturated with NBDM at concentrations higher than 40 μM (Figure 1A). The observed saturation suggests that the conjugate is taken up through facilitated diffusion and that uptake inhibition could be a result of transporter saturation. A sigmoidal plot of NBDM uptake is indicative of a cooperative binding of NBDM conjugate with transporters, with an affinity constant of $K_a = (22 \pm 1.4) \mu\text{M}$ (SigmaPlot 12.2). Furthermore, we observed that transported NBDM remains in the cells even after repeated washing. This observation is in agreement with previous observations in which 2,5-anhydro-D-mannitol was found to be a suitable substrate for a number of kinases such as phosphofruktokinase-1.^[16] This lack of back-transport is a significant point because Glut transporters, being antiporters, take up and excrete carbohydrates, but not the phosphorylated products.^[17]

The uptake of NBDM was compared with that of NBDF and NBDG (Figure 1). We observed that NBDF was transported half as effectively as NBDM. Enhanced NBDM uptake can be interpreted in terms of the preference of the transporter for the cyclic furanose mimic over the furano/pyrano mixture of fructose conformers, as has previously been recognized for 2,5-anhydro-D-mannitol versus fructose.^[7a] Comparison of the uptake of NBDF/NBDM conjugates with that of glucosamine showed that regardless of the increased relative conformational flexibil-

ity of NBDG, its uptake exceeded that of the fructosamine or manitolamine conjugates. On the basis of these findings, we suggest that Holman's observations of inhibition of fructose uptake by manitolamine derivatives were the result of competitive uptake as opposed to merely binding. It is noteworthy that the ratio of NBDG/NBDF uptake correlates with the ratio measured previously for ^{14}C -labeled analogues of glucose and fructose,^[18] thus underlining that NBD conjugates are reliable probes for evaluating carbohydrate uptake.

NBDM as a fructose-transporter-specific probe

Fructose uptake by the cell occurs through several transporters, out of which Glut5 is a fructose-specific transporter, whereas Glut2 has affinity for both fructose and glucose.^[2a] To determine whether NBDM is a competitive substrate for fructose transporters, NBDM uptake

was evaluated in the presence of increasing concentrations of fructose. In view of Holman's demonstration that 1-amino-2,5-anhydro-D-mannitol analogues exhibit high inhibitory constants against fructose uptake, it was hypothesized that low concentrations of fructose would not interfere with NBDM uptake. Indeed, uptake of NBDM was unchanged with fructose concentrations ≤ 0.1 mM. Supplementation of NBDM solution with 0.01 mM glucose, on the other hand, resulted in up to threefold uptake enhancement (Figure 2A). In contrast to NBDM, fructose/glucose supplementation had a relatively moderate effect on NBDG uptake.

High concentrations of fructose and glucose inhibited uptake in a substrate-specific manner (Figure 2B). NBDG uptake was thus inhibited both by fructose and by glucose at 1–50 mM concentrations. In contrast, NBDM uptake was inhibited only by fructose, and not by glucose, at high concentrations. The inhibitory constant for fructose was determined by least squares fitting to the Michaelis–Menten equation and by nonlinear regression analysis as 2.77 mM or 2.3 mM, respectively (Figure 2C, D). The kinetic analysis considered decay in NBDM-induced fluorescence (ΔV) derived as $V_0 - V$, where V_0 and V are NBDM uptake in the absence and in the presence of fructose, respectively.

The difference in the results obtained for fructose and for glucose reflects the specificity of the NBD conjugate. Thus, if occurring through nonspecific transporters,^[2b,3] NBDM uptake

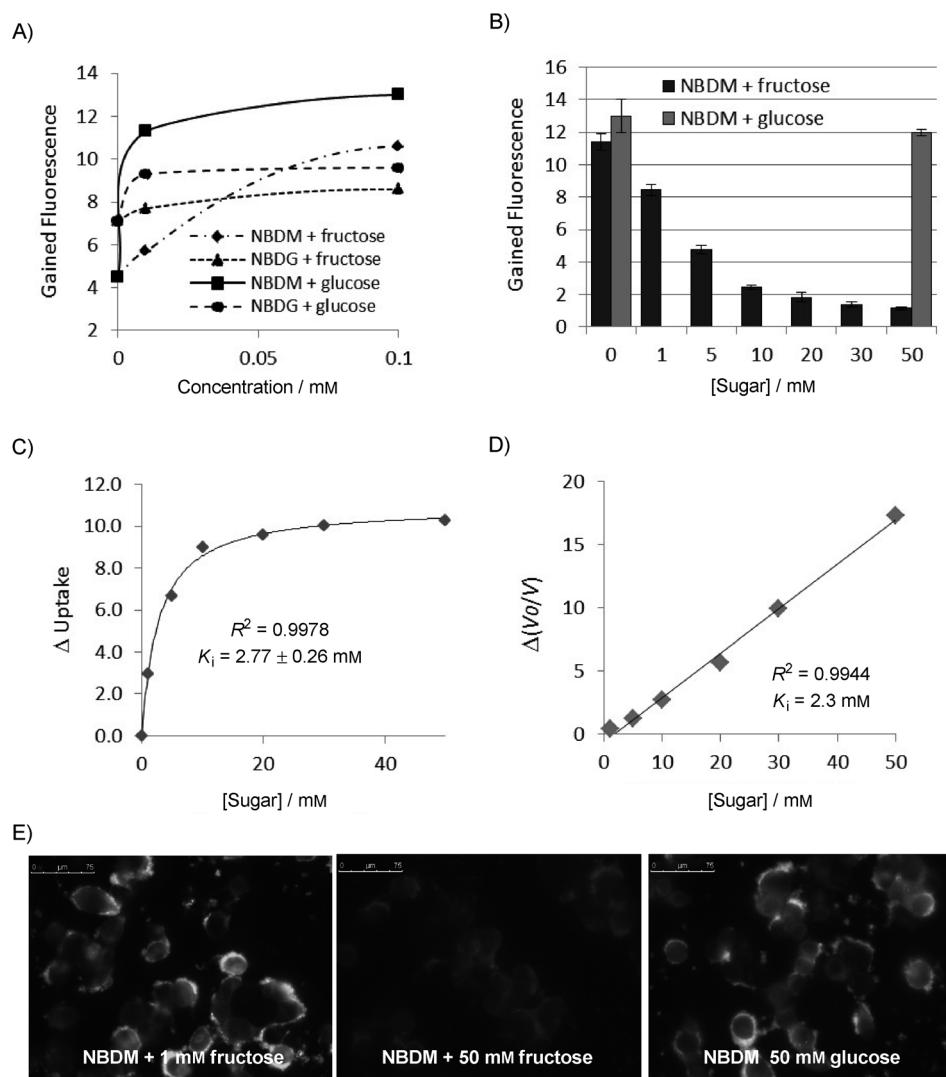


Figure 2. Impact of carbohydrates on NBDM uptake in MCF7 cells. A) NBDM uptake is enhanced at low concentrations of glucose and fructose. B) NBDM uptake inhibition by fructose but not by glucose. C) Fructose-induced NBDM fluorescence inhibition. The K_i value was calculated by least squares fitting to the Michaelis–Menten equation. D) Nonlinear regression analysis of inhibitory effect of fructose on NBDM uptake. V_0 and V : calculated velocities of NBDM uptake at 0–50 mM fructose over 15 min. E) Fluorescence images showing the effect of 50 mM fructose and 50 mM glucose on NBDM-treated MCF7 cell fluorescence. Uptake studies were carried out with 10 μ M NBDM in PBS supplemented with 0.01 mM glucose. Note: gray regions appear fluorescent green in color images.

would be expected to diminish in the presence of either fructose or glucose. In contrast, NBDM uptake is inhibited solely by fructose and not by glucose, suggesting a preferential uptake of NBDM through a fructose-specific transporter. For the NBDG probe, however, uptake is diminished by both carbohydrates.

THF-based fructose-mimetic and fructose-specific transport

Of the nonspecific fructose transporters (Glut2 and potentially Glut7, Glut9, and Glut11), Glut2 has relatively low affinity for fructose.^[19] Localization analysis by immunocytochemistry showed that both Glut2 and Glut5 are present in the membranes and in the cytoplasm of MCF7 cells;^[20] however, functional data suggests that the levels of each isoform in the

membranes vary depending on the cell line. Data obtained with [¹⁴C]-D-fructose and cytochalasin B, a mycotoxin known to have an inhibitory effect on glucose transport,^[21] have shown that Glut2 contributes \approx 12% to the total fructose uptake across the membranes of MCF-7 cells.^[9]

The previously mentioned fructose-mediated inhibition and preconditioning studies (Figure 2) strongly suggest that NBDM is transported preferentially through the action of Glut5, but we conjectured that the possibility of Glut2 involvement in NBDM uptake should be determined experimentally. Glut2 facilitates uptake of glucose, fructose, and also glucosamine, in the last case with an affinity 21 times higher than that for glucose (0.8 vs. 17 mM, respectively).^[3b] To evaluate the role of Glut2 in the uptake of NBDM, uptake of NBD conjugates in the presence of glucosamine as a competitive inhibitor was measured. The resulting data are summarized in Figure 3. We observed that glucosamine, at a concentration as low as 0.01 mM, inhibits NBDM uptake: 50 mM glucosamine inhibits NBDM uptake by 25%. With NBDG, glucosamine appears to play a dual role, facilitating uptake at low concentrations (< 1 mM) and inhibiting uptake at high concentrations (> 1 mM).

An increase in glucosamine concentration from 1 mM to 50 mM thus induced a drop of \approx 9% in the influx of NBDG. In contrast to NBDM and NBDG, glucosamine does not impact NBDM uptake even at concentrations as high as 50 mM.

The observed inhibition of NBDM and NBDG uptake by glucosamine suggests that both conjugates are substrates for the same transporter: namely Glut2. Conversely, the lack of NBDM uptake inhibition by glucosamine suggests that NBDM is not a substrate for Glut2-mediated uptake. We propose that the origin of this difference is in sugar conformation, with Glut5 recognizing and transporting sugars in their furanose forms^[7a] and Glut2 recognizing and transporting sugars in their pyranose forms. According to this model, the lack of NBDM uptake through Glut2 can be explained by the fact that 1-amino-2,5-anhydro-D-mannitol is locked in the furanose form. Although

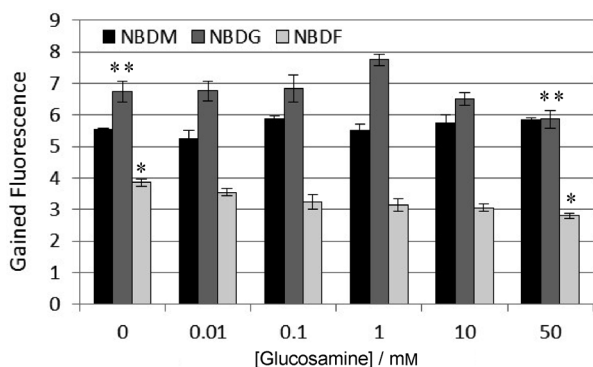


Figure 3. Impact of glucosamine on NBD conjugate uptake in MCF7 cells. Fluorescence was measured with an eGFP filter set (excitation 450/490 nm, emission 515/565 nm) after treatment of cells with 10 μ M NBD in PBS supplemented for 15 min. Data represent the gained fluorescence as sums of intensity for selected cells (10–15) measured in duplicate. Statistical analysis was performed by use of the t-test: two-sample assuming equal variances. * $P(T \leq t)$ two-tail = 0.008; ** $P(T \leq t)$ two-tail = 0.001 ($\alpha = 0.05$).

this model might be tested in future studies using locked fructopyranose analogues, the observed results indicate that Glut5 has a strong preference for transporting furanose rings over their pyranose counterparts and that we have identified the first Glut5-specific fluorescent probe. Access to this Glut5 specific probe should enable us and others to investigate what environmental factors influence transport through Glut5 and to measure Glut5-specific transport across tissue types better.

Preconditioning with fructose enhances NBDM uptake

The specificity of the NBDM probe towards fructose-specific transporters was further evaluated in MCF7 cells by measuring uptake into cells grown in media with or without fructose. As a control, NBDG was used to evaluate the impact of fructose preconditioning on expression/activation of nonspecific fructose/glucose transport. We observed that fructose preconditioning impacts NBDM uptake but not NBDG uptake (Figure 4). Cells grown in, for example, a fructose-rich medium—that is, preconditioned with fructose—for four days transported twice as much NBDM as cells grown in a standard medium (Figure 4A, MCF7* vs. MCF7). In contrast, no significant changes in NBDG uptake were detected upon fructose preconditioning. Starving cells of fructose, by maintaining them in a medium supplemented with dialyzed FBS for four days, resulted in a 2.5-fold decrease in NBDM uptake (Figure 4A, MCF7' vs. MCF7). Notably, starved MCF7 cells were also less efficient than the control cells in taking up NBDG (Figure 4A, MCF7* vs. MCF7', $p < 0.01$). Lastly, when fructose-starved cells were then preconditioned with fructose, the cells transported NBDM as effectively as control cells (Figure 4A, MCF7 vs. MCF7'* and MCF7 vs. MCF7'*).

These data are consistent with prior observations relating to fructose preconditioning/starvation. Preconditioning of Caco2 cells in dialyzed serum and hexose-free media, for example, resulted in lower expression of Glut5, and this effect was reversed after fructose and glucose were replenished.^[22] In addition,

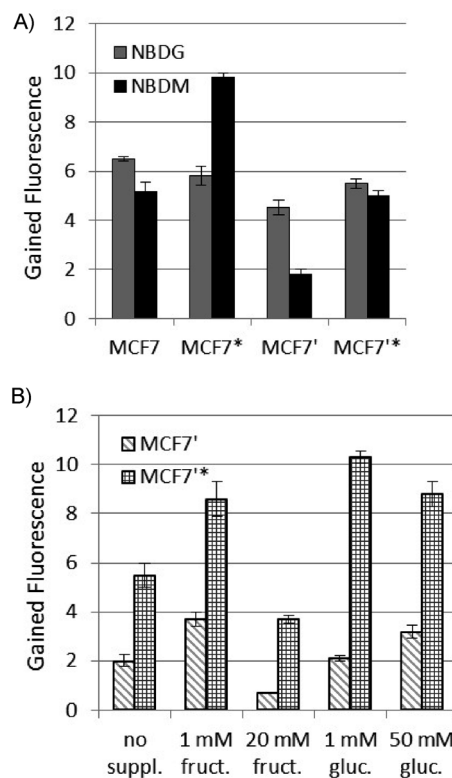


Figure 4. Uptake of NBD conjugates in MCF7 cells preconditioned with or without fructose. A) Fructose preconditioning modulates NBDM uptake. B) NBDM uptake in the presence of fructose (fruct.) or glucose (gluc.). MCF7: cells grown in standard medium (RPMI + 10% FBS + 1% streptomycin/ampicillin). MCF7*: cells grown in standard medium supplemented with 11 mM fructose. MCF7': cells grown in dialyzed medium (RPMI + 10% dialyzed FBS). MCF7'*: cells grown in dialyzed media supplemented with 11 mM fructose. Data represent the Gained Fluorescence as sums of intensity for selected cells (10–15) measured in duplicate.

tion, the levels of transporter expression were found to be modulated by a carbohydrate-rich diet. With respect to fructose transporters, a fructose-enriched diet increased Glut5 levels in the small intestine and kidney of fructose-fed rats.^[23] Fructose feeding also contributed to expression of the Glut2 transporter, although to a lesser degree than of Glut5.^[23]

NBDM uptake was inhibited by high concentrations of fructose regardless of whether the cells were preconditioned with or starved of fructose (Figure 4B). Thus, when 20 mM fructose was added to the cells with NBDM, decreases in NBDM uptake of more than twofold were observed in both MCF7' and MCF7'* sets of cells. As expected, glucose did not inhibit NBDM uptake even at 50 mM concentration. In addition, consistently with the previous experiments (Figure 4B), low concentrations of fructose or glucose facilitated NBDM uptake in the fructose-preconditioned MCF7'* set of cells. In the MCF7' cells (MCF7 cells grown in dialyzed medium), however, enhancement in NBDM uptake was observed only with low concentrations of fructose.

These observations suggest that fructose preconditioning regulates fructose transporter expression—an observation consistent with previous reports.^[22,23] We propose that the differ-

ential impact of fructose preconditioning on NBDM versus NBDG uptake indicates that NBDM uptake is most likely facilitated by a fructose-specific transporter such as Glut5. This Glut5-based transport model is supported by the observation that similar NBDG uptake was observed both in control MCF7 cells and in MCF7* cells; fructose feeding thus appears to impact fructose-specific transport, whereas nonspecific fructose transport is unaffected. The moderate loss of NBDG uptake observed for the MCF7* cells suggests that starving cells of fructose and other non-glucose hexoses, typically provided by nondialyzed FBS, has an impact on the expression/function of nonspecific transport involved in the uptake of fructose, glucose, and other carbohydrates.

NBDM as a probe for comparing Glut5 efficiency amongst cell lines

Our data collected thus far indicate that NBDM is transported through the action of fructose-specific transporters, thus suggesting its potential application as a probe to evaluate differential activity/expression of Glut5 between cell lines. As a proof of principle, we have evaluated NMBD in normal (184B5) breast cells and compared the results to those observed with MCF7. The NBDG probe was also evaluated to reflect total levels of glucose and nonspecific fructose transport in 184B5 versus MCF7 cells (Figure 5).

After comparative evaluation of NBDM in MCF7 versus 184B5 cells, we found that NBDM can effectively distinguish between the two cell lines. MCF7 cells transported approximately four times more NBDM than 184B5 cells. In contrast, the uptake of NBDG by these two cell lines differed by less than twofold. In the context of an observed specificity of NBDM towards Glut5, these data indicate a significant difference between cancer MCF7 and normal 184B5 cells in expression/activity of Glut5, whereas differential uptake of NBDG

reflect the total change in glucose transporters, including non-specific glucose/fructose Gluts.

The increased expression of the fructose-specific transporter Glut5 in cancer cells relative to normal cells is well documented. Zamora-Leon and co-workers, for instance, have shown that breast carcinoma cell lines MCF-7 and MDA-MB-231 have greater levels of Glut5 mRNA and protein, and exhibit higher rates of fructose transport, than normal and human breast cancers.^[20] This finding was confirmed in later Glut5 knockdown studies (MCF-7 and MDA-MB-231 cells) in which fructose uptake was diminished and cell proliferation and growth were inhibited.^[24] A screening of the Glut family of transporters in malignant versus normal human tissues and cells showed that Glut5 was overexpressed in 27% of cancerous tissues tested, including brain, breast, colon, liver, lung, testis, and uterus tumors.^[25] In separate studies evaluating Glut5 expression at the mRNA level, Gambhir et al. observed that MCF7 cells were, unexpectedly, ten times lower in Glut5-coding mRNA than their normal immortalized counterparts (MCF10A) while still transporting twice as much fructose as MCF10A cells.^[18] It was suggested that this discrepancy arose from fructose influx through alternative fructose transporters such as Glut7, -9, or -11, and not Glut5.

The apparent preference of NBDM for fructose-specific transport strongly suggests that Glut5 is the most likely route of fructofuranose uptake. Furthermore, it appears that nonspecific fructose transporters such as Glut2, -7, -9, or -11 that take up both glucose and fructose^[25,26] play a minor role in fructose transport, contributing mostly to the influx of fructopyranosides. Gambhir's observation of low Glut5 mRNA levels and high observed fructose uptake, combined with Cheeseman's observations that Glut5 protein expression is high (Western blotting), indicates that regulation of Glut5 is complex.^[26a] Little is known with regard to post-transcriptional regulation of Glut5 expression and the mechanisms that control cellular

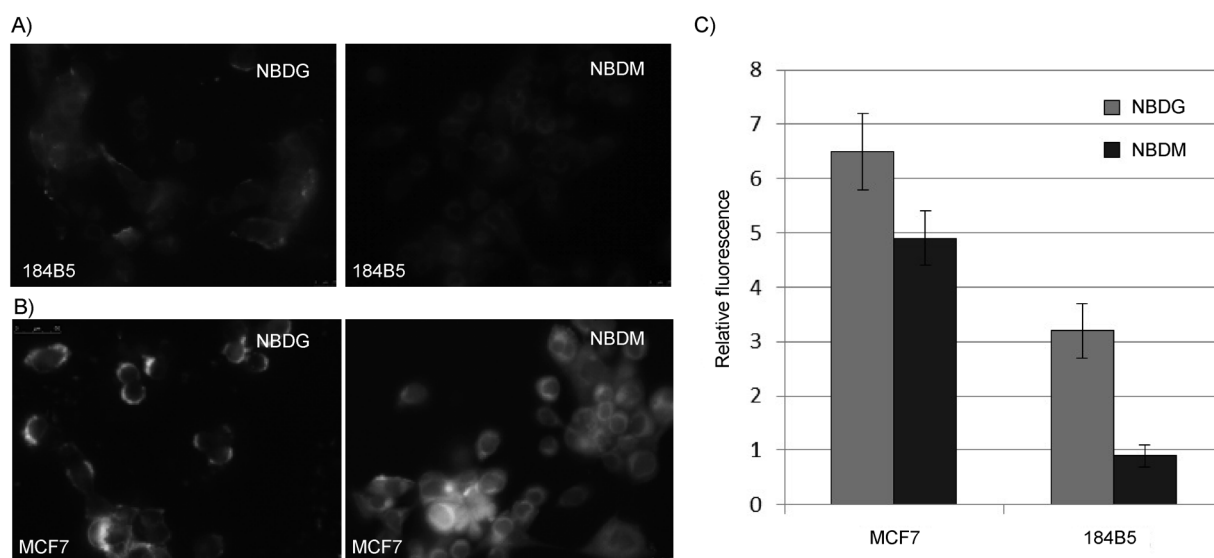


Figure 5. NBD conjugates exhibit enhanced uptake in cancer cells. A) 184B5 cells and B) MCF7 cells treated with NBDG and NBDM. C) Quantified uptake data showing a preference for NBDM uptake by MCF7 cells (ca. fourfold enhanced uptake). Note: gray regions appear fluorescent green in color images.

membrane localization. The Cheeseman/Gambhir dichotomy suggests that control over fructose uptake is more sophisticated than control over mRNA transcription.

Conclusions

Cellular carbohydrate influx is controlled by transporters that recognize structural features of carbohydrates. The data obtained in this study indicate that fluorescently labeled 1-amino-2,5-anhydro- β -mannitol (NBDM) is transported twice as efficiently as fructose. Inhibition of NBDM uptake by fructose, but not by glucose or glucosamine, indicates that the probe is transported through a path that is independent of Glut1 and Glut2. From the data presented here, the best model for the transport of NBDM is through the fructose-specific transporter Glut5. The outcome of these studies, in conjunction with previous observations, provides evidence that molecular recognition of fructose by fructose-specific versus nonspecific transporters could be governed by the furanose/pyranose conformational equilibrium. The preference of Glut5 for the furanose form, the observed fructose-transport-specific uptake of NBDM, and the differential uptake in cancer cells versus normal cells provide evidence that functionalized THF derivatives can serve as Glut5 probes for direct comparative evaluation of the functional fructose-specific transporter between cell types.

Experimental Section

Chemical synthesis of NBDM: A mixture of 1-amino-2,5-anhydro- β -mannitol (20 mg, 12.3 mmol), NBDCl (30 mg, 14.8 mmol), and NaHCO₃ (50 mg, 60 mmol) in MeOH/H₂O (4:1, v/v, 1.5 mL) was stirred at 55 °C for 5 h with shielding from light. The reaction mixture was centrifuged (1 min at 15000 rpm) to precipitate residual solids. The remaining solution was concentrated and taken up in the minimum possible amount of MeCN. The product, NBDM, was isolated by preparative TLC with a mixture of MeCN/H₂O 17:3 (*R_f* = 0.68). NBDM was obtained as an orange solid in 58–62% yield. For cell studies, NBDM was purified by HPLC with a Phenomenex C18 column [Luna 5u C18(2) 100A, 250×4.60 mm, 5 micron] and MeOH/H₂O as a mobile phase (gradient from 5% to 50% MeOH over 10 min, flow 1 mL min⁻¹). ¹H NMR (600 MHz, CD₃OD): δ = 8.48 (d, *J* = 9.4 Hz, 1H), 6.54 (d, *J* = 9.0 Hz, 1H), 4.26 (m, 3H), 4.01 (t, *J* = 5.5 Hz, 1H), 3.96 (d, *J* = 5.1 Hz, 1H), 3.91 (d, *J* = 4.8 Hz, 1H), 3.59 (dd, *J* = 12.0, 3.4 Hz, 1H), 3.59 ppm (dd, *J* = 11.7, 5.3 Hz, 1H); ¹³C NMR (150 MHz, CD₃OD): δ = 147.2, 146.4, 146.3, 136.9, 122.9, 122.9, 103.9, 85.7, 83.0, 80.9, 78.7, 63.2, 58.0 ppm; HRMS (ESI⁻): calcd. for C₁₂H₁₃N₄O₇: 325.0784 [M-H]⁻; found: 325.0828.

Cell culture: MCF7 cells and 184B5 cells (ATCC) were seeded from the frozen cultures in 10 cm dishes at 37 °C under 5% CO₂/90% air. MCF7 cells were grown and further maintained in RPMI 1640 medium supplemented with heat-inactivated FBS (10%) and ampicillin/streptomycin (1%, "standard" growth medium). 184B5 cells were grown and further maintained in 10 cm dishes in MEM medium supplemented with FBS (15%) and antibiotics (ampicillin and streptomycin, 1%). MCF7 cells were passaged with trypsin every three days, and 184B5 cells were passaged with trypsin every five days. The medium was changed 12 h after seeding.

For fructose preconditioning studies, MCF7 cells, grown in the standard growth medium, were passaged and maintained in: 1) the standard medium supplemented with fructose (final concentration 11 mM), and 2) in RPMI-1640 medium supplemented with dialyzed FBS (10%) and ampicillin/streptomycin (1%). The medium was changed 24 h after passaging of cells and every two days thereafter.

Fluorescence studies: Cells at 90% confluence were collected with trypsin, plated in 35 mm MatTek glass-bottomed dishes (10000/plate), and left for 10 h. After 10 h, trypsin-containing medium was removed, and the cells were supplemented with fresh medium and left for another 10 h. The cells were then washed once with PBS and treated with NBD in PBS (10 μ M) at 37 °C for 15 min. After incubation, cells were washed with cold PBS (3×1 mL). Fluorescent images were obtained with live cells and a Leica TCS SPE high-resolution spectral confocal microscope with an eGFP filter set (excitation 450/490 nm, emission 515/565 nm) and tenfold objective. Data were quantified with the Leica Application Suite software. Single-cell imaging and confocal microscopy was performed with a Nikon TE2000-E2 Eclipse microscope (Nikon Instruments, Inc., Melville, NY, USA), imaged with a CoolSNAP HQ2 monochrome camera (Photometrics) and 40-fold lens, and analyzed with Nikon NIS Elements software. Z-stack imaging of cells stained with wheat germ agglutinin/Alexa

Fluor 594 to distinguish the outer membrane from the cytosol allows rejection of optical signatures arising from electrostatic association of NBD with the cell surface. Microscopes were each equipped with a live cell chamber at 5% CO₂, 30% humidity to maintain constant conditions during the experiment. Cells were analyzed in triplicate by the integrated intensity of the fluorescent signature. Fluorescence was normalized by calculating the fold increase of the net cell fluorescence with respect to background autofluorescence.

Acknowledgements

We acknowledge the Susan G. Komen for the Cure foundation (M.T. postdoctoral fellowship), the National Cancer Institute (Grant CA123007), the NSF (CHE 1152020, M.P. and D.T.M.), and FSU-CRC (M.E.M. and G.F.S.) for supporting this research. We warmly thank Professor Martin Loessner (ETH, Laboratory of Food Microbiology) for providing access to the Leica TCS SPE high-resolution spectral confocal microscope and FSU facility for training.

Keywords: breast cancer · carbohydrates · fluorescent probes · fructose transport · Glut5

- [1] a) L. Tappy, K. A. Le, *Physiol. Rev.* **2010**, *90*, 23–46; b) A. R. Gaby, *Altern. Med. Rev.* **2005**, *10*, 294–306.
- [2] a) A. R. Manolescu, K. Witkowska, A. Kinnaird, T. Cessford, C. Cheeseman, *Physiology* **2007**, *22*, 234–240; b) V. Douard, R. P. Ferraris, *Am. J. Physiol. Endocrinol. Metab.* **2008**, *295*, E227–E237.
- [3] a) T. Kayano, C. F. Burant, H. Fukumoto, G. W. Gould, Y. S. Fan, R. L. Eddy, M. G. Byers, T. B. Shows, S. Seino, G. I. Bell, *J. Biol. Chem.* **1990**, *265*, 13276–13282; b) M. Uldry, M. Ibberson, M. Hosokawa, B. Thorens, *FEBS Lett.* **2002**, *524*, 199–203.
- [4] a) D. Hanahan, R. A. Weinberg, *Cell* **2000**, *100*, 57–70; b) D. Hanahan, R. A. Weinberg, *Cell* **2011**, *144*, 646–674.
- [5] R. L. Wahl, G. D. Hutchins, D. J. Buchsbaum, M. Liebert, H. B. Grossman, S. Fisher, *Cancer* **1991**, *67*, 1544–1550.

- [6] T. Haradahira, A. Tanaka, M. Maeda, Y. Kanazawa, Y. I. Ichiya, K. Masuda, *Nucl. Med. Biol.* **1995**, *22*, 719–725.
- [7] a) A. Tatibouët, J. Yang, C. Morin, G. D. Holman, *Bioorg. Med. Chem.* **2000**, *8*, 1825–1833; b) J. Girmiene, A. Tatibouët, A. Sackus, J. Yang, G. D. Holman, P. Rollin, *Carbohydr. Res.* **2003**, *338*, 711–719.
- [8] G. D. Holman, W. D. Rees, *Biochim. Biophys. Acta Biomembr.* **1982**, *685*, 78–86.
- [9] B. J. Trayner, T. N. Grant, F. G. West, C. I. Cheeseman, *Bioorg. Med. Chem.* **2009**, *17*, 5488–5495.
- [10] J. Yang, J. Dowden, A. Tatibouët, Y. Hatanaka, G. D. Holman, *Biochem. J.* **2002**, *367*, 533–539.
- [11] R. Weissleder, V. Ntziachristos, *Nat. Med.* **2003**, *9*, 123–128.
- [12] a) K. Yoshioka, H. Takahashi, T. Homma, M. Saito, K. B. Oh, Y. Nemoto, H. Matsuoka, *Biochim. Biophys. Acta Gen. Subj.* **1996**, *1289*, 5–9; b) K. Yoshioka, M. Saito, K. B. Oh, Y. Nemoto, H. Matsuoka, M. Natsume, H. Abe, *Biosci. Biotechnol. Biochem.* **1996**, *60*, 1899–1901; c) J. Levi, Z. Cheng, O. Gheysens, M. Patel, C. T. Chan, Y. B. Wang, M. Namavari, S. S. Gambhir, *Bioconjugate Chem.* **2007**, *18*, 628–634.
- [13] J. T. Bagdanoff, M. S. Donoviel, A. Nouraldein, J. Tarver, Q. Fu, M. Carlsson, T. C. Jessop, H. Zhang, J. Hazelwood, H. Nguyen, S. D. Baugh, M. Gardyan, K. M. Terranova, J. Barbosa, J. Yan, M. Bednarz, S. Layek, L. F. Courtney, J. Taylor, A. M. Digeorge-Foushee, S. Gopinathan, D. Bruce, T. Smith, L. Moran, E. O'Neill, J. Kramer, Z. Lai, S. D. Kimball, Q. Liu, W. Sun, S. Yu, J. Swaffield, A. Wilson, A. Main, K. G. Carson, T. Oravec, D. J. Augeri, *J. Med. Chem.* **2009**, *52*, 3941–3953.
- [14] S. Claustre, F. Bringaud, L. Azema, R. Baron, J. Perie, M. Willson, *Carbohydr. Res.* **1999**, *315*, 339–344.
- [15] P. Zancan, M. Sola-Penna, C. M. Furtado, D. Da Silva, *Mol. Genet. Metab.* **2010**, *100*, 372–378.
- [16] a) T. A. Koerner, Jr., E. S. Younathan, A. L. Ashour, R. J. Voll, *J. Biol. Chem.* **1974**, *249*, 5749–5754; b) F. M. Raushel, W. W. Cleland, *J. Biol. Chem.* **1973**, *248*, 8174–8177; c) W. L. Dills, T. R. Covey, P. Singer, S. Neal, M. S. Rappaport, *Carbohydr. Res.* **1982**, *99*, 23–31.
- [17] L. Azema, S. Claustre, I. Alric, C. Blonski, M. Willson, J. Perie, T. Baltz, E. Tetaud, F. Bringaud, D. Cottem, F. R. Opperdoes, M. P. Barrett, *Biochem. Pharmacol.* **2004**, *67*, 459–467.
- [18] G. Gowrishankar, S. Zitzmann-Kolbe, A. Junutula, R. Reeves, E. Levi, A. Srinivasan, K. Bruus-Jensen, J. Cyr, L. Dinkelborg, S. S. Gambhir, *PLoS One* **2011**, *6*, e26902.
- [19] C. I. Cheeseman, *Gastroenterology* **1993**, *105*, 1050–1056.
- [20] S. P. Zamora-León, D. W. Golde, I. I. Concha, C. I. Rivas, F. Delgado-López, J. Baselga, F. Nualart, J. C. Vera, *Proc. Natl. Acad. Sci. USA* **1996**, *93*, 1847–1852.
- [21] C. Y. Jung, A. L. Rampal, *J. Biol. Chem.* **1977**, *252*, 5456–5463.
- [22] J. Mesonero, M. Matosin, D. Cambier, M. J. Rodriguez-Yoldi, E. Brot-Laroche, *Biochem. J.* **1995**, *312*, 757–762.
- [23] C. F. Burant, M. Saxena, *Am. J. Physiol. Gastrointest. Liver Physiol.* **1994**, *267*, G71–G79.
- [24] K. K. Chan, J. Y. Chan, K. K. Chung, K. P. Fung, *J. Cell. Biochem.* **2004**, *93*, 1134–1142.
- [25] A. Godoy, V. Ulloa, F. Rodriguez, K. Reinicke, A. J. Yanez, L. Garcia Mde, R. A. Medina, M. Carrasco, S. Barberis, T. Castro, F. Martinez, X. Koch, J. C. Vera, M. T. Poblete, C. D. Figueroa, B. Peruzzo, F. Perez, F. Nualart, *J. Cell. Physiol.* **2006**, *207*, 614–627.
- [26] a) Q. Li, A. Manolescu, M. Ritzel, S. Yao, M. Slugoski, J. D. Young, X. Z. Chen, C. I. Cheeseman, *Am. J. Physiol. Gastrointest. Liver Physiol.* **2004**, *287*, G236–G242; b) H. Doege, A. Bocianski, A. Scheepers, H. Axer, J. Eckel, H. G. Joost, A. Schürmann, *Biochem. J.* **2001**, *359*, 443–449.

Received: March 20, 2013

Published online on June 19, 2013